Characterization of Inner Retinal Hyperreflective Alterations in Early Cognitive Impairment on Adaptive Optics Scanning Laser Ophthalmoscopy

Yi Stephanie Zhang,[1] Alex C. Onishi,[1] Nina Zhou,[1] Jessica Song,[1] Sahej Samra,[1] Sandra Weintraub,[2,3] and Amani A. Fawzi[1]

[1]Department of Ophthalmology, Feinberg School of Medicine, Northwestern University, Chicago, Illinois, United States
[2]Mesulam Center for Cognitive Neurology and Alzheimer's Disease, Feinberg School of Medicine, Northwestern University, Chicago, Illinois, United States
[3]Department of Psychiatry and Behavioral Sciences, Feinberg School of Medicine, Northwestern University, Chicago, Illinois, United States

Correspondence: Amani A. Fawzi, Department of Ophthalmology, Feinberg School of Medicine, Northwestern University, 645 North Michigan Avenue, Suite 440, Chicago, IL 60611, USA; afawzimd@gmail.com.

Submitted: April 3, 2019
Accepted: July 5, 2019

Citation: Zhang YS, Onishi AC, Zhou N, et al. Characterization of inner retinal hyperreflective alterations in early cognitive impairment on adaptive optics scanning laser ophthalmoscopy. *Invest Ophthalmol Vis Sci*. 2019;60:3527–3536. https://doi.org/10.1167/iovs.19-27135

Purpose. To examine inner retinal hyperreflective features on adaptive optics scanning laser ophthalmoscopy (AOSLO) in individuals with early cognitive impairment.

Methods. In this prospective, cross-sectional study, we enrolled 12 participants with either amnestic mild cognitive impairment (aMCI, $n = 10$) or early dementia due to Alzheimer's disease (eAD, $n = 2$) and 12 age-, sex-, and race-matched cognitively normal controls. All participants completed AOSLO imaging of the inner retina. AOSLO montages of the peripapillary area were graded for hyperreflective features including granular membranes, mottled membranes, and nummular features. Regions of interest on AOSLO were compared qualitatively to corresponding optical coherence tomography (OCT) cross sections. OCT was also used to analyze peripapillary retinal nerve fiber layer (RNFL) thickness.

Results. Cognitively impaired individuals had a significantly higher number of granular membranes with a larger overall area compared to controls. The proportion of cognitively impaired individuals with two or more granular membranes was 41.7% compared to none in the control group. Granular membrane area was also inversely correlated with cognitive performance on the Montreal Cognitive Assessment. There was no difference between the two groups in terms of other membrane types or RNFL thickness.

Conclusions. Individuals with early cognitive impairment related to Alzheimer's show hyperreflective granular membranes on high-resolution imaging, which we hypothesize to be manifestations of inner retinal gliosis. The presence of these subtle hyperreflective membranes may obscure underlying RNFL thinning in these eyes on OCT imaging. The distinctive phenotype of granular membranes surrounding the optic nerve on AOSLO may represent a new potential biomarker of early Alzheimer's.

Keywords: adaptive optics scanning laser ophthalmoscopy, aoslo, cognitive impairment, alzheimer's disease, gliosis

Alzheimer's disease (AD) is a neurodegenerative disease with hallmark extracellular amyloid plaques that involve not only the brain but also the inner retina.[1] The inner retina bears the brunt of pathology, confirmed by histopathological studies that identified optic nerve axon degeneration and macular loss of retinal ganglion cells (RGCs) in the eyes of patients with AD.[2,3]

Before the onset of dementia due to AD, patients may be identified as having mild cognitive impairment (MCI) based on neurocognitive testing.[4] Those with amnestic type MCI (amnestic mild cognitive impairment [aMCI]) have up to a 48.7% chance of converting to AD within 30 months and thus represent an important target population for early intervention and disease surveillance.[5] Several studies have examined inner retinal changes on optical coherence tomography (OCT) in individuals with MCI in hopes of finding early biomarkers of the disease.[6–9] However, results have been highly variable, showing decreased,[6] unremarkable,[9] or increased[7] retinal nerve fiber layer (RNFL) thickness in MCI. Interestingly, in AD individuals with more advanced cognitive impairment, RNFL thinning is a universal finding, suggesting that this may be a late finding in these eyes.[6,8]

One potential explanation for the wide variability in RNFL measurements could be related to the occurrence of reactive gliosis in the inner retina in MCI and early stages of AD.[10] We hypothesize that gliosis in these early stages may mask underlying subtle RNFL thinning on OCT since hypertrophy and proliferation of glial cells both within and on the surface of the RNFL may lead to artifactual thickening of the RNFL.[7,11] Gliosis is a common inflammatory response involving hypertrophy, proliferation, and functional changes in glial cells in response to stress.[12] This response has been reported in the brain and eye in chronic neurodegenerative diseases such as Parkinson's disease and AD and in glaucoma.[13–15] Histopatho-

logical studies of AD have reported reactive astrocytes clustered around amyloid-β (Aβ) plaques in the brain[14] and increased glial cell number and reactivity in the retina.[3,12] In primary open-angle glaucoma, presumed activated retinal astrocytes and Müller cells appear on OCT as patchy hyperreflective structures on the RNFL that may mask RNFL thinning.[15,16]

Hyperreflective retinal alterations that may suggest gliosis have not been studied in vivo in the eyes of those with AD-related dementia or in MCI. Recent advancements in adaptive optics scanning laser ophthalmoscopy (AOSLO) allow noninvasive visualization of the RNFL in vivo.[17] This technique reveals inner retinal features at resolutions that are not possible with OCT.[17,18] Scoles et al.[18] have used AOSLO to characterize seven categories of hyperreflective inner retinal structures in participants with neurological diseases other than AD. In this prospective case–control study, we used AOSLO to investigate hyperreflective signatures in a population with early cognitive impairment (aMCI or early dementia due to AD (eAD) and compared them to cognitively normal, matched controls.

Methods

Study Population

This single-center case–control study at the Department of Ophthalmology, Northwestern University in Chicago, Illinois, was prospectively approved by the Institutional Review Board of Northwestern University. The study was conducted in accordance with the tenets of the Declaration of Helsinki. We used the University of California, San Diego Brief Assessment of Capacity to Consent (UBACC) to assess capacity to provide informed consent and obtained written informed consent from all participants.

We recruited a total of 16 cognitively impaired individuals with a clinical diagnosis of aMCI[4] ($n = 14$ participants) or eAD[19] ($n = 2$ participants) and 14 matched cognitively normal controls from the Clinical Core of the Northwestern Alzheimer's Disease Center (ADC). We combined aMCI and eAD participants in this cohort because of the presumed shared underlying cause of their cognitive impairment and similar severity of impairment (mild).[4] We specifically focused on aMCI participants, defined as MCI individuals with a predominant memory domain deficit.

The clinical diagnoses of aMCI and eAD were based on previously published diagnostic criteria from the National Institute on Aging.[4,19] Briefly, all aMCI and eAD diagnoses required a detailed research clinical assessment to rule out additional medical causes of impairment and a formal neuropsychological battery from the Uniform Data Set (UDS) as described in the Cognitive Assessment section. Whenever possible, available biomarker data were also included in consideration of the final diagnosis.[4,19] The ADC provided available cerebral spinal fluid (CSF) biomarker status, determined based on $A\beta_{1-42}$ and phosphorylated-tau levels as previously described,[20] and apolipoprotein E ε4 (apoE4) allele status, a genetic risk factor of AD.[21] AD patients were required to meet criteria for dementia and additionally to have insidious onset of disease and cognitive deficits in amnestic and nonamnestic domains on testing that were characteristic for dementia caused by AD. Our aMCI and eAD participants were required to have Montreal Cognitive Assessment (MoCA) ≥ 13 (Mini-Mental State Exam [MMSE]) equivalent of ≥ 19)[22] to be categorized as early in their disease course. In addition to specific neurocognitive performance metrics, the diagnosis of MCI required preservation of activities of daily living while eAD required an impairment of activities of daily living due to the cognitive loss. Thus, all participants had a study partner who completed the Activities of Daily Living Questionnaire, a reliable assessment of functional ability in dementia.[23,24] Cognitively normal controls also underwent the same battery of assessments. Control individuals were matched to the cognitively impaired individuals based on age (within 3 years), sex, and race.

Exclusion criteria included pre-existing ocular pathology such as glaucoma, macular degeneration, diabetic or hypertensive retinopathy, retinal detachment, ocular trauma, high myopia (>6 diopters [D]), intraocular pressure (IOP) of >20, epiretinal membranes or extensive cataracts confirmed by participant report, OCT images, and review of electronic medical records. Participants meeting any of these exclusion criteria by personal report, OCT images, or on review of medical records were excluded. We also excluded participants with neurological disorders known to affect the retina such as multiple sclerosis and Parkinson's disease, as well as conditions such as uncontrolled hypertension or diabetes, and current smokers. On AOSLO, we excluded eyes that had less than one quadrant imaged or poor-quality images with the RNFL not in focus. On OCT, we excluded images with a signal quality measure of <6 or an absolute signal strength intensity <45.

Cognitive Assessment

All participants had completed the same extensive annual neurocognitive assessment using the Uniform Data Set (UDS) of the National Institute on Aging Alzheimer's Disease Program.[25] Testing included a battery of clinical, functional, and neuropsychological assessments in the domains of language, visuospatial functions, executive attention, and working memory.[25] In the current study, we focused on memory domain tests including the Craft Story 21 immediate and delayed recall, which assess episodic memory, and the Rey Audio Verbal Learning Test delayed recall, which assesses word list memory. The MoCA is also included as a measure of overall cognitive function. We also report the global score on the Clinical Dementia Rating (CDR) scale, a clinical metric of cognitive–functional impairment. Amnestic MCI is usually defined by a global CDR score of 0.5 and eAD by a score of 0.5 to 1.0 (mild dementia).[26] On all reported neuropsychological tests, a higher score indicates better performance.

Ophthalmologic Assessment

We obtained a full history and reviewed the electronic health record of all participants for past medical, ocular, surgical, and medication (including eye drops) history that may suggest a confounding ocular disease such as glaucoma. All participants underwent manual refraction, best-corrected visual acuity, confrontational visual field testing, and IOP measurement using Tono-Pen (Reichert Technologies, Buffalo, NY, USA). All imaging was performed after pupil dilation (proparacaine 0.5%, tropicamide 1%, and phenylephrine 2.5% ophthalmic solutions). Macular and optic nerve pathology was assessed on OCT scans by a board-certified ophthalmologist, retina specialist (A.A.F.).

Adaptive Optics Imaging

We acquired AOSLO images using the Apaeros LF retinal imaging system (Boston Micromachines Corporation, Boston, MA, USA) based on the optical design of Dubra et al.[27] As previously described,[28] the system uses an 97 actuator AlpAO DM (AlpAO SAS, Montbonnot, France) with 25 μm of stroke for wavefront correction. The light sources include two superluminescent diodes, centered at 790 and 850 nm. The 790-nm

source was used in imaging and the 850-nm source for wavefront sensing. The combined power at the eye was ~130 μW.

Our AOSLO images were focused on the inner retina, specifically the inner surface of the RNFL, which was identified by the characteristic reflective retinal nerve bundle striations and vasculature as previously shown.[17,18] We began image acquisition at the optic nerve head and continued in a grid pattern, guided by a widefield mirror to capture the superior, temporal, and inferior peripapillary regions. We started with widefield 5° × 4.5° image sequences of the RNFL layer for orientation, then acquired 2° × 2° scans. In areas of interest, we also obtained additional high-resolution 1° × 1° images. Images were acquired in sequences of 60 frames over 2 seconds. To facilitate montaging, we used an overlap of 0.5° between image sequences.

Optical Coherence Tomography Imaging

We acquired structural RNFL thickness using the RTVue-XR OCT Avanti System (Optovue, Inc., Fremont, CA, USA. Software Version 2016.1.0.26). We also examined the peripapillary 4.5 × 4.5-mm^2 en face OCT and cross-sectional B-scans qualitatively for inner retinal pathology corresponding to regions of interest on AOSLO.

Adaptive Optics Image Analysis

We uploaded the AOSLO images onto ImageJ[29] and extracted representative frames (individual images from the image sequence) of each region of the RNFL for semiautomated montage of the individual frames using the i2k Retina Pro montaging software (DualAlign LLC, Clifton Park, NY, USA). Two separate graders (Y.S.Z., A.C.O.), masked to the diagnosis of the participants, identified hyperreflective features on the montages. They categorized the features based on their size, location, and phenotypic appearance and measured their area and dimensions. In addition, we measured the total retinal area imaged in each participant. All measurements were performed on Image J and calculated based on a theoretical (not actual) average axial length of 24 mm.

Membrane Types

Membranes with previously reported characteristics were categorized based on specifications by Scoles et al.[18] Granular membranes were defined as a contiguous hyperreflective structure >50 μm in diameter with texture similar to clustered grains of sand, forming a mesh-like membrane with distinct borders. Nummular features were defined as a discrete disc-shaped hyperreflectivity 10 to 30 μm in diameter. Membranes that did not fit into previously reported types were named by agreement. For example, we identified mottled membranes that did not fit into either the waxy—noted as a very smooth and opaque membrane— or granular membranes described by Scoles et al.[18] We defined mottled membranes as >50 μm in diameter and obscuring the underlying RNFL with some areas of clearing. Their texture was coarser compared to waxy or granular membranes, nonhomogeneous, and speckled with scattered punctate areas of reflectivity >10 μm in diameter.

Statistical Analysis

All statistical analyses were performed using SPSS24 (IBM Corp., Armonk, NY, USA). An interclass correlation (ICC) for absolute agreement was performed for the image analysis results completed by the two separate graders. A P value of <0.05 was considered significant for all analyses. We used the Mann-Whitney U test for nonparametric comparison of the number and area covered by hyperreflective membranes between the cognitively normal and impaired groups as well as between the CSF biomarker or apoE4 allele present and absent group. We used Fisher's exact test for small sample sizes to compare the proportion of individuals in each group (cognitively impaired or control) with membranes. Spearman correlation for nonparametric populations was used to investigate the correlation between membrane parameters and cognitive performance or age. We did not compare nummular features between our cohorts as these features are prevalent in both healthy and diseased states.[18]

Results

Our study originally recruited 30 participants (aMCI $n = 14$, eAD $n = 2$, control $n = 14$ participants). One aMCI individual was excluded for inability to follow the target to complete imaging. Two aMCI and two control participants were excluded for bilateral poor image quality, likely due to extensive cataracts. Finally, one aMCI individual was excluded for findings of intraretinal edema on OCT. Ultimately, 10 aMCI and 2 eAD participants were eligible for further analysis. Six individual eyes (5 eyes due to poor image quality, 1 eye for fixation difficulties) were excluded, leaving 18 eyes in the cognitively impaired group for final analysis. In the 12 control participants, 3 eyes were excluded due to poor image quality, leaving 21 eyes as shown on Table 1.

Overall, the number of eyes and the peripapillary area successfully imaged were not significantly different between the two groups. Of note, only 5/12 of the cognitively impaired and 10/12 of the control participants had complete imaging of the superior quadrant of the optic nerve due to machine limitations. Other demographic information shows that the two groups were successfully matched according to age, sex, and race and had similar IOP and interval between cognitive testing and imaging visits. As expected, the cognitively impaired group performed worse on all cognitive tests.

The two graders showed excellent absolute ICC with coefficient of 0.930 (95% confidence interval [CI] at 0.831–0.971). A total of 26 membranes were found in our 24 participants (39 total eyes). Most of the membranes (20/26) were found in the inferior quadrant while 2 granular membranes were found in the temporal quadrant and 4 granular membranes were found in the superior quadrant of eyes with aMCI. Table 2 summarizes the overall results for hyperreflective membranes and RNFL thickness. Table 3 summarizes the correlation between membrane parameters and participant age or cognitive score.

Available apoE4 data were obtained from 21 participants. Seven of the 12 (58.3%) cognitively impaired individuals had at least 1 apoE4 allele while none of the 9 controls with available genetic data had any apoE4 alleles. Five of our cognitively impaired participants had CSF biomarker data available and were all biomarker positive. When considering the genetic and biomarker data together, nine (75%) cognitively impaired participants had at least one apoE4 allele or CSF biomarker present. Thirteen of the remaining participants had no genetic allele or CSF biomarkers. Table 4 summarizes our findings comparing membrane parameters between the cohort with either genetic allele or CSF biomarker present and the participants with both parameters absent.

Granular Membranes

Figure 1 shows representative images of granular membranes. On AOSLO, the granular membranes showed a sand-like

Investigative Ophthalmology & Visual Science

Table 1. Demographics and Cognitive Information

Characteristics	aMCI/eAD, $n = 12$	Control, $n = 12$	*P* Value*
Sex, male/female	3/9	3/9	
Age, y†	71.92 ± 5.87	72.66 ± 6.43	0.98
Education, y†	16.12 ± 2.33	16.83 ± 1.64	0.59
Race, *n*			
African American	1	1	
Caucasian/Hispanic	9/2	11/0	
Diabetes, *n*§	1	0	
Hypertension, *n*§	4	3	
IOP, mm Hg†	16.08 ± 2.91	16.58 ± 2.19	0.59
No. of eyes imaged†	1.50 ± 0.52 (18 total)	1.75 ± 0.45 (21 total)	0.32
Area of eye imaged, mm^2†	8.52 ± 4.96	12.09 ± 8.12	0.38
Interval between cognitive and imaging visits, y†	0.386 ± 0.261	0.269 ± 0.190	0.20
MoCA, total = 30†	22.08 ± 3.70	26.92 ± 2.15	**<0.001**
CDR†‡	0.54 ± 0.14	0 ± 0	**<0.001**
CS Imm, total = 25†	9.75 ± 2.73	17.50 ± 2.39	**<0.001**
CS Del, total = 25†	6.33 ± 5.58	16.50 ± 3.03	**<0.001**
RAVLT Del, total = 15†	2.91 ± 4.01	10.75 ± 3.31	**<0.001**

Statistically significant *P* values are bold. CS Imm, Craft Story immediate; CS Del, Craft Story delayed; RAVLT Del, Rey Auditory Verbal Learning Test delayed recall.

* 2-tailed *P* values from Mann-Whitney *U* test.

† Data reported as mean ± standard deviation.

‡ CDR scores range from 0 (no dementia) to 0.5 (questionable) to 1.0 (mild).

§ Participants with uncontrolled diabetes or hypertension or with retinopathy related to medical disease were excluded.

texture and did not follow the direction of the RNFL. The membranes covered the RNFL, most often adjacent to the vasculature. On Figure 2, corresponding areas on OCT cross sections (Figs. 2G–I) showed that a minority of granular membranes (4/21 membranes, 19.0%) could be visualized on OCT as preretinal hyperreflective layers, while the majority of membranes were not discernable on OCT. Four of the aMCI participants with granular membranes also had noncontiguous, poorly defined satellite hyperreflective lesions surrounding the primary well-demarcated granular membrane, as shown in Figures 1B and 1E in blue arrows.

We found that in the group with cognitive impairment, 7/12 (58.3%) participants had granular membranes (19 membranes total) while only 2/12 (16.7%) control participants had granular membranes (2 membranes total), as summarized in Table 2. We found that a statistically significant ($P = 0.037$) proportion of cognitively impaired individuals had more than one granular membrane (2+ membranes) as compared to the control group, with a large effect size of Cramer's V = 0.513. However, there was no difference in the number of participants in either group with one membrane or more (1+ membrane). We also found that the cognitively impaired group had more membranes ($P =$

Table 2. Comparison of RNFL Thickness and Membrane Parameters Between the Cognitively Impaired and Control Groups

AOSLO or OCT Parameter	aMCI/eAD, $n = 12$	Control, $n = 12$	*P* Value
All membranes			
Total No. of membranes	22	4	
Participants with 1+ membrane(s)	7/12	3/12	0.21*
Participants with 2+ membranes	5/12	1/12	0.16*
Mean No.†	1.83 ± 0.705	0.330 ± 0.188	0.056‡
Mean area† mm^2	0.0943 ± 0.0425	0.0275 ± 0.0266	0.066‡
Granular membrane			
Total No. of membranes	19	2	
Participants with 1+ membrane(s)	7/12	2/12	0.19*
Participants with 2+ membranes	5/12	0/12	**0.037***
Mean No.†	1.58 ± 0.609	0.167 ± 0.112	**0.020‡**
Mean area† mm^2	0.0833 ± 0.0379	0.00163 ± 0.00119	**0.020‡**
Mottled membrane			
Total No. of membranes	3	2	
Participants with 1+ membrane(s)	2/12	1/12	1*
Mean No.†	0.250 ± 0.179	0.167 ± 00.167	0.58‡
Mean area† mm^2	0.0110 ± 0.00808	0.0534 ± 0.0534	0.62‡
RNFL thickness			
Global† μm	98.82 ± 3.48	99.29 ± 3.74	0.67‡
Inferior quadrant† μm	130.07 ± 4.39	127.13 ± 5.55	0.88‡

Statistically significant *P* values are bold.

* 2-tailed *P* values using Fisher's exact test.

† Data reported as mean ± standard error.

‡ 2-tailed *P* values using Mann-Whitney *U* test.

Investigative Ophthalmology & Visual Science

Table 3. Spearman Correlation Between Membrane Parameters, Cognitive Performance, and Age

Membrane Parameter	MoCA		Age	
	r Value	*P* Value	*r* Value	*P* Value
Total membranes				
No.	−0.294	0.163	−0.254	0.230
Area	−0.326	0.121	−0.325	0.122
Granular membranes				
No.	−0.376	0.07	−0.159	0.459
Area	**−0.411**	**0.046**	−0.220	0.302
Mottled membranes				
No.	0.017	0.938	−0.143	0.505
Area	−0.012	0.955	−0.153	0.476

Statistically significant *P* values are bold.

0.020; Hedges' g effect size = 0.902) and wider area covered by granular membranes ($P = 0.020$; Hedges' g effect size = 0.879) compared to the controls.

Table 3 summarizes a statistically significant inverse correlation ($r = -0.411$, $P = 0.046$) between the overall extent of granular membranes and cognitive performance in the entire cohort. We found that individuals with a larger area of granular membranes had worse performance on the MoCA. Lastly, while Table 4 shows no statistically significant differences between participants with genetic or CSF biomarkers and those without, the cohort with apoE4 or CSF biomarker present had a higher mean number ($P = 0.051$) and area ($P = 0.060$) of granular membranes that was approaching significance.

Mottled Membranes

Figures 3A and 3B show mottled membranes, which were found in the cognitively impaired ($n = 2$ participants) and control ($n = 1$ participant) groups. Mottled membranes showed a coarse and lacy appearance with scattered and larger punctate areas of hyperreflectivity, often appearing nonhomogeneous, which distinguished them from granular membranes. All of the mottled membranes were found in the inferior quadrant. There were no corresponding alterations visualized on OCT. We did not find a statistically significant difference in these membranes between the cognitively normal and impaired groups or between the CSF biomarker or apoE4 allele present and absent groups.

Nummular Features

We found clusters of nummular hyperreflective features (Figs. 3C, 3D) in both aMCI ($n = 4$ participants) and control ($n = 4$ participants) individuals. These disc-shaped granular textured reflective features appeared on the inner retina with a diameter of 10 to 30 μm and often had a central clearing, as previously described.[18]

Discussion

The major finding of our study is that individuals with early cognitive impairment related to suspected AD have more numerous and larger areas covered by granular membranes, which we hypothesize are manifestations of inner retinal gliosis on AOSLO. These membranes (up to 500 μm in diameter) are much larger than the solid ovoid retinal amyloid plaques (1–10 μm) that have previously been reported in AD histopathological studies.[1,30] We hypothesize that these preretinal granular membranes (Fig. 1) could be a manifestation of reactive gliosis, related either to Müller cell end feet that normally form the internal limiting membrane, activated glial cells that have migrated to a location of stress,[31] or reactive astrocytic processes that normally surround blood vessels in the inner retina. Previous studies have established an association between AD and glial cell activation in the brain and retina.[3,13] In the human AD retina, Blanks et al.[3] described extensive labeling of Müller cell radial processes and end feet in addition to proliferation and activation of astrocytes. Furthermore, an animal model of AD has shown histologically dense bundles of Müller cell end feet forming a network surrounding the blood vessels of the inner retina.[32] In the MCI population, our group previously found an inverse correlation between RNFL thickness in the inferior quadrant and cognitive performance, leading us to hypothesize that reactive gliosis may be an earlier feature than previously observed.[3,7]

Many studies have explored whether RNFL measurements could serve as an early marker for detection of AD.[7,9,33,34] However, the results of these studies have been highly controversial, showing either thinner, unremarkable, or thicker RNFL measurements in MCI participants compared to controls.[7,9,33,34] In the current cohort, we found no difference in RNFL thickness between the cognitively impaired and control groups (Table 2). This finding corroborates our prior study[7] and further supports the hypothesis that reactive gliotic changes in early cognitive impairment may mask or precede pathological neurodegeneration that is ultimately detectable in later stages of AD as RNFL thinning.[6,33] If the initial change in the retina of cognitively impaired individuals is indeed reactive gliosis, then this may explain the highly variable reports of RNFL changes in MCI groups[6,7,9] and would call for a paradigm shift in the search for retinal biomarkers that could be ideal for early detection.

Our current study highlights granular membranes, a potential manifestation of gliosis on AOSLO, as a candidate

Table 4. Comparison of Membrane Parameters Between the apoE4 or CSF Present and Absent Groups

Membrane Parameter	apoE4 or CSF Biomarker Present, *n* = 9	apoE4 or CSF Biomarker Absent, *n* = 13	*P* Value*
Granular membrane			
Total No. of membranes	17	4	
Mean No.†	1.875 ± 0.772	0.308 ± 0.175	0.051
Mean area† mm^2	0.0818 ± 0.0446	0.0218 ± 0.0728	0.060
Mottled membrane			
Total No. of membranes	3	2	
Mean No.†	0.333 ± 0.236	0.154 ± 0.154	0.601
Mean area† mm^2	0.0147 ± 0.0106	0.0493 ± 0.0493	0.647

* 2-tailed *P* values from Mann-Whitney *U* test.
† Data reported as mean ± standard error.

Investigative Ophthalmology & Visual Science

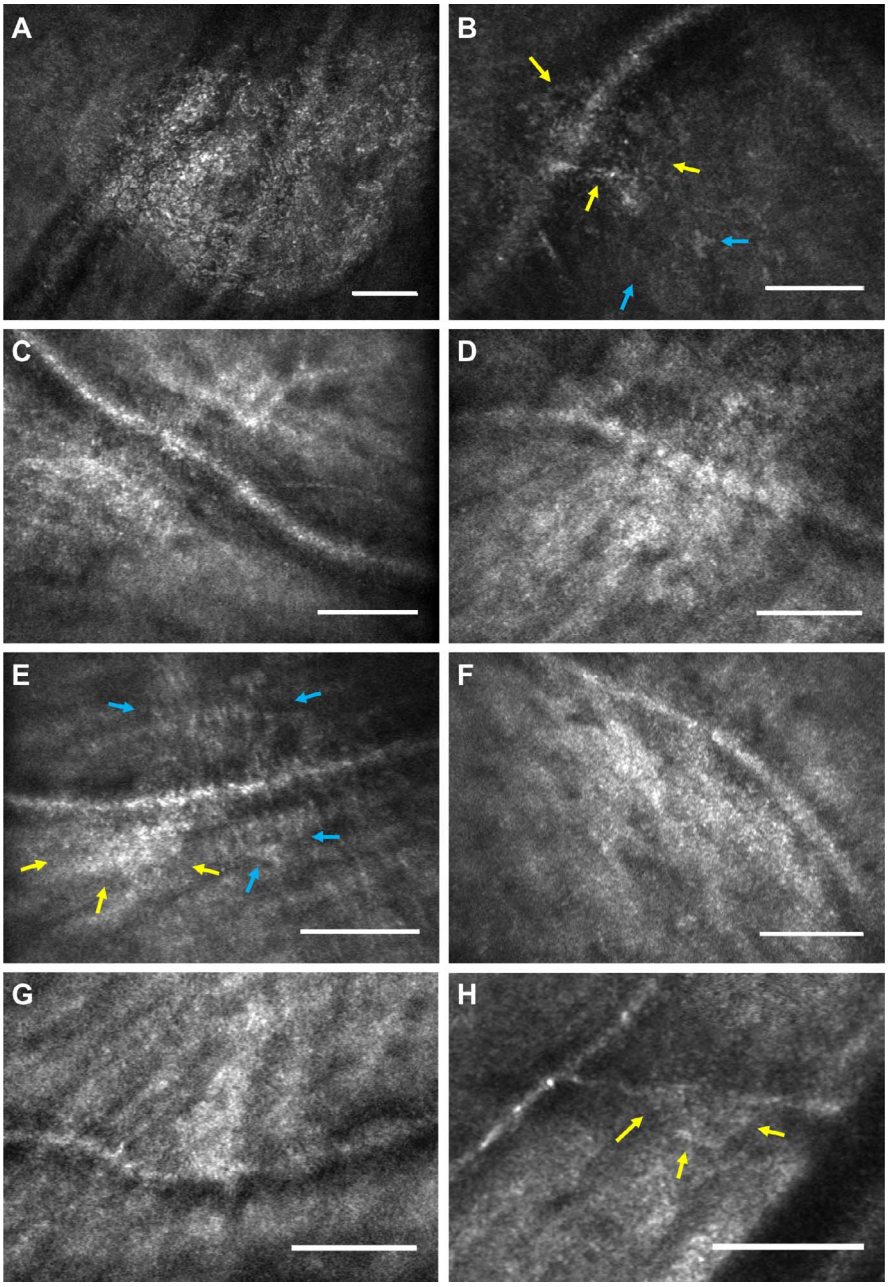

Figure 1. Granular membranes on adaptive optics scanning laser ophthalmoscopy (AOSLO). *Scale bars*: 100 µm. (**A**–**F**) AOSLO en face images of granular membranes from cognitively impaired participants; (**G**, **H**) granular membranes from controls. *Yellow arrows* help delineate the primary granular membrane. In (**B**, **E**), the *blue arrows* delineate the satellite lesions.

biomarker for early cognitive impairment. Another avenue for biomarkers is the retinal vasculature, which can be visualized noninvasively by OCT angiography (OCTA).[35] Several groups have found decreased parafoveal vessel density and flow on OCTA in those with more advanced AD, especially in rigorous studies that accounted for potential age-related changes.[36,37] According to the vascular hypothesis of AD, early hypoperfusion in AD may lead to decreased Aβ clearance and subsequent plaque accumulation,[38,39] and thus, vascular alterations could be early manifestations in the course of the disease. Indeed, our group recently showed that individuals with early cognitive impairment also exhibit inner retinal hypoperfusion that manifests on OCTA as decreased parafoveal vessel density.[40] Our current finding of granular membranes on AOSLO and previous study of vascular hypoperfusion on OCTA provide promising biomarkers of early AD that warrant large-scale investigations.

A secondary finding in our study is an association between granular membrane area and poor cognitive performance (Table 3), which further suggests that these membranes may serve as biomarkers. However, longitudinal studies are needed to further investigate the relationship between these membranes and conversion to AD or disease progression. It is possible that the satellite lesions seen in a few aMCI and eAD participants are secondary extensions of gliosis that may eventually become contiguous components of the primary granular membrane, a question to be explored in longitudinal studies.

Investigative Ophthalmology & Visual Science

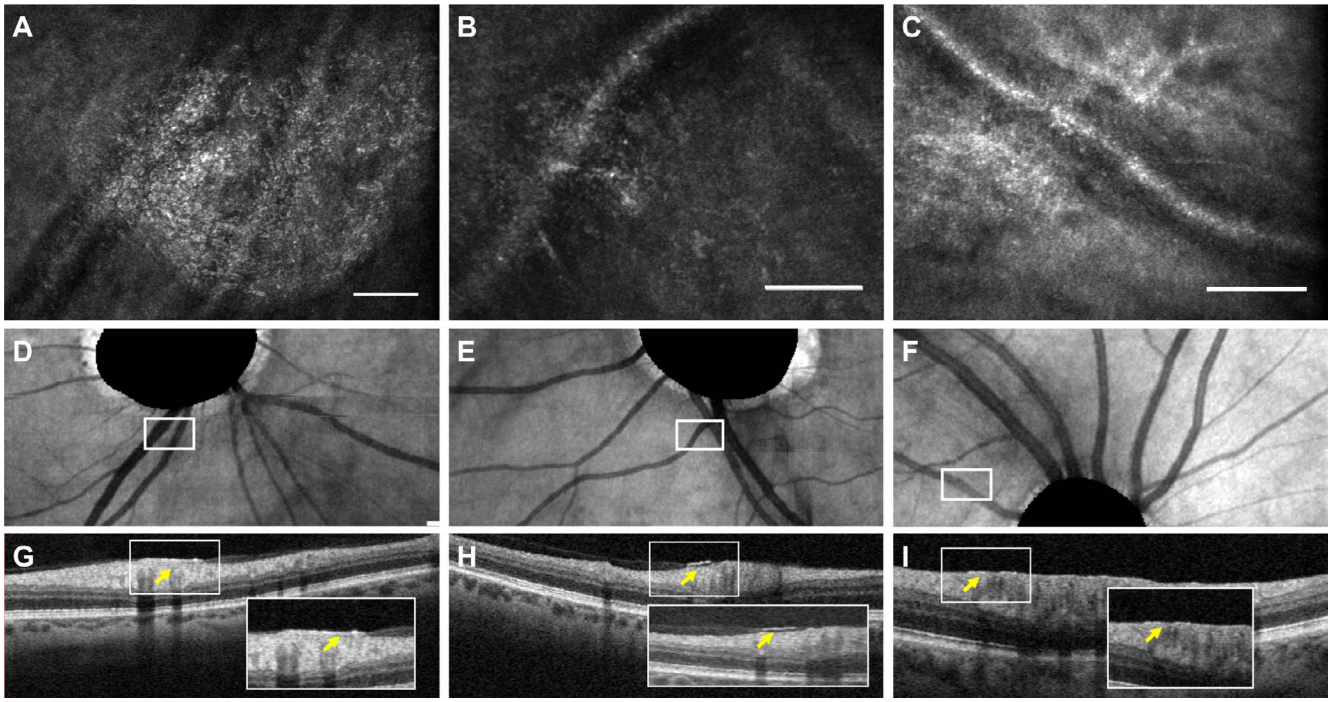

Figure 2. Granular membranes on multimodal imaging. *Scale bars*: 100 µm. (**A–C**) Adaptive optics scanning laser ophthalmoscopy (AOSLO) en face images of granular membranes. (**D–F**) The corresponding location of the AOSLO membranes highlighted in *white boxes* on en face optical coherence tomography (OCT). The OCT images show masked optic nerve heads as automated by the machine. (**G–I**) The OCT B-scans in the corresponding region of interest. The cross sections in (**G**, **H**) with their insets illustrate subtle hyperreflective features above the retina (*yellow arrow*), while in (**I**) there is a suggestion of focal thickening of the internal limiting membrane (*yellow arrow*).

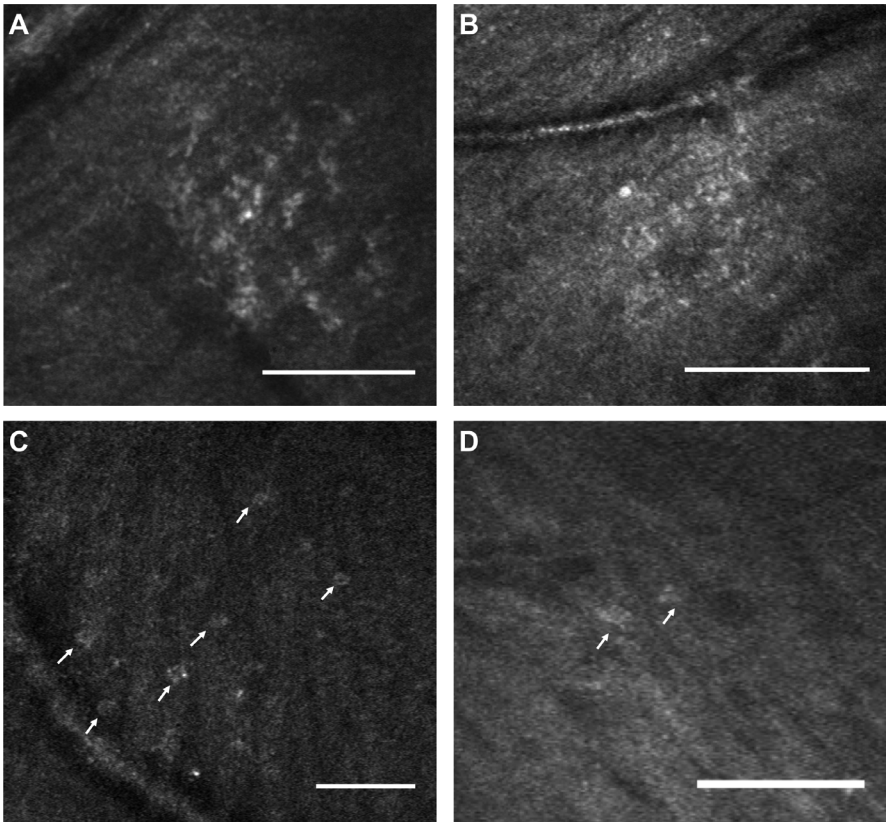

Figure 3. Mottled membranes and nummular features on adaptive optics scanning laser ophthalmoscopy (AOSLO). *Scale bars*: 100 µm. (**A**, **B**) Representative AOSLO en face images of mottled membranes from controls. (**C**, **D**) AOSLO en face nummular features from cognitively impaired individuals.

Investigative Ophthalmology & Visual Science

We also found a trend toward significantly increased number and area of granular membranes in participants with either the apoE4 allele or CSF biomarkers of AD, a trend that did not exist for mottled membranes. ApoE is a cholesterol carrier that has been implicated in Aβ metabolism. The apoE4 allele is one of the strongest genetic risk factors for AD, with the odds ratio of developing disease reported to range from 14.9 to 33.1 in individuals with two alleles.[21,41,42] CSF biomarker positivity provides indirect evidence of AD pathology in MCI and AD patients, with a positive predictive value for conversion to AD of 60% to 70% in individuals with MCI.[43,44] Therefore, individuals with either the apoE4 allele or CSF biomarkers represent a high-risk population for having or developing AD pathology. The trend of increased granular but not mottled membrane parameters in these high-risk individuals further supports the potential role of granular membrane in bolstering current biomarker and genetic data to risk stratify patients. Future studies correlating AOSLO findings to complete Alzheimer's biomarker data should be considered.

Beyond our findings in cognitively impaired individuals, our study reflects on the relevance of exploring the inner retina using AOSLO. Previously, hyperreflective alterations superficial to the RNFL on OCT have been putatively linked to activated glial cells in diseases such as glaucoma[16,45] and retinitis pigmentosa,[46] and in normal aging.[16,47] AOSLO has a much higher lateral resolution than OCT, allowing for more specific characterization of the surface features of these hyperreflective structures,[18] which is critical in illustrating their pathological signatures. For example, on AOSLO epiretinal membranes appear striated and contracted,[48] while waxy membranes appear smooth like dripped wax.[18] Both of these membranes are phenotypically distinct from the granular or mottled membranes described in our study, a fine distinction that far exceeds the resolution possible on OCT. In fact, the majority of our membranes (22/26 membranes, 84.6%) showed no corresponding alterations on cross-sectional OCT. Thus, our study highlights the importance of using AOSLO, to better define the phenotypic and pathological spectrum of inner retinal hyperreflective signatures.

On AOSLO, Scoles et al.[18] previously showed that granular membranes can be seen in several disease states including glaucoma and Parkinson's, where histopathological evidence of gliosis in the retina has been reported.[13,49,50] Therefore, we believe that granular membranes could be a manifestation of a common gliotic pathway shared by several disease entities. Our data (Table 2) showed that a greater proportion of cognitively impaired participants had multiple granular membranes ($n = 5$ participants, 41.7%) compared to controls ($n = 0$ participants). Although a small minority of controls ($n = 2$ participants, 16.7%) also had granular membranes, they each had a single small membrane. The presence of membranes in our control group is not surprising when considering the many pathways that lead to gliotic changes. In fact, hyperreflective alterations can be found on OCT in healthy eyes, especially with advancing age.[16,45,47] Perhaps taking into account the number and extent of membranes rather than the presence of a single small membrane may be an important consideration in future studies exploring granular membranes as biomarkers.

In our study, we intentionally excluded patients with ocular pathology such as retinal detachment and glaucoma that may be associated with gliosis. We also found no significant correlation between age and membrane parameters, suggesting that the hyperreflective alterations seen in our cognitively impaired group cannot be explained by aging. The granular membranes were mostly found near vessels around the optic disc and not associated with any contraction, distinguishing them from epiretinal membranes that have a distinctive striated and contracted appearance on AOSLO.[48,51] However, based on our data, we were not able to determine the status of posterior vitreous adherence in our participants. Thus, we were unable to comment on the possible contribution of the vitreous to our findings, which may be interesting to consider for future studies.

Other hyperreflective alterations found in both groups include nummular reflective features that have previously been found in both healthy and pathological retinas.[18] They were hypothesized to be Gunn's dots or physiological Müller glial cell end feet.[18] We also found mottled membranes with no difference (number or size) between the two groups. Our data suggest that the distinction between granular and mottled membranes, made possible by AOSLO, appears to be important in the study of AD.

Our study paves the way for future AOSLO investigations of inner retinal hyperreflective alterations as potential new biomarkers of early AD. Our findings also serve as a window into early disease pathophysiology involving potential gliosis. As the number of individuals living with AD is projected to grow from 55 million to 88 million by 2050, it is critically important to better understand early disease pathophysiology in order to identify biomarkers that are noninvasive and predictive of disease progression.[52] Current CSF and positron emission tomography markers are invasive and costly, and lack the sensitivity and specificity for early disease detection.[53–55] On the other hand, AOSLO is noninvasive and has the ability to capture inner retinal pathology at unparalleled high resolutions in vivo.[17] Future studies with a larger sample size and longitudinal design will be essential to validate AOSLO as a tool for screening, surveillance, or risk stratification of patients with early cognitive impairment. The results of these studies could help identify a subgroup within the mildly cognitively impaired population that is at higher risk for progression to AD,[4] who could be ideal candidates for early therapeutic intervention.[53]

The strengths of our study include the prospective matched (age, sex, and race) control design. In addition, our control group underwent an equally rigorous neurocognitive assessment as the cognitively impaired group. The rigor and reproducibility of our AOSLO data analysis was ensured by two independent masked graders, and the excellent ICC. The biggest limitation of our study is our small sample size, which can be attributed to the stringent patient selection criteria as well as strict image quality requirements. As the average age of our study population was over 70, the presence of cataracts or inability of patients to fixate on the target for the duration of imaging affected AOSLO image quality, which limited complete collection of AOSLO data in all participants. However, the large effect size of our findings, despite the small sample size, suggests that there is a meaningful difference between the cognitively impaired and control groups. Other limitations include technical limitations that precluded superior quadrant image acquisition in all our participants. Since the superior quadrant is thought to be most affected by AD pathology,[56] data from this quadrant may have further strengthened our results. Furthermore, technical limitations in superior quadrant imaging stand as a temporary and technically surmountable limitation in the current system that should not be construed as a generalized limitation of the AOSLO approach in future studies. We also did not obtain axial length for correction of magnification error. However, given the relatively large size of membranes and the exclusion of high myopes, we would not expect our results to change significantly with axial length corrections. Lastly, we were unable to obtain biomarker data from all of our participants.

In conclusion, we found significantly more granular membranes, hypothesized to be manifestations of gliosis, in the early cognitively impaired group than in their cognitively normal counterparts. Moreover, increasing granular membrane area correlated with worsening cognitive performance. Over-

all, our study suggests that individuals with early cognitive impairment related to AD have granular membranes on AOSLO, not detectable on OCT, that may represent a potentially early noninvasive marker of AD. Future directions include studies with larger sample sizes as well as longitudinal studies to examine the ability of these retinal hyperreflective changes to predict future cognitive decline and conversion to AD.

Acknowledgments

The authors thank Peter Nesper and Hee Eun Lee from the Department of Ophthalmology at Northwestern for helping with image acquisition and Mallory Ward from the Mesulam Center for Cognitive Neurology and Alzheimer's Disease for providing participant referrals.

Supported by the Illinois Society for the Prevention of Blindness, National Institutes of Health Grant DP3DK108248 (AAF), and National Institutes of Health Grant NIA-AG13584 (Northwestern Alzheimer's Disease Core Center). The authors alone are responsible for the content and writing of the paper. AOSLO instrument support was provided by Boston Micromachines Corporation.

Disclosure: **Y.S. Zhang**, None; **A.C. Onishi**, None; **N. Zhou**, None; **J. Song**, None; **S. Samra**, None; **S. Weintraub**, None; **A.A. Fawzi**, None

References

1. Koronyo Y, Biggs D, Barron E, et al. Retinal amyloid pathology and proof-of-concept imaging trial in Alzheimer's disease. *JCI Insight*. 2017;2:e93621.
2. Blanks JC, Torigoe Y, Hinton DR, Blanks RH. Retinal pathology in Alzheimer's disease. I. Ganglion cell loss in foveal/parafoveal retina. *Neurobiol Aging*. 1996;17:377–384.
3. Blanks JC, Schmidt SY, Torigoe Y, Porrello KV, Hinton DR, Blanks RH. Retinal pathology in Alzheimer's disease. II. Regional neuron loss and glial changes in GCL. *Neurobiol Aging*. 1996;17:385–395.
4. Albert MS, DeKosky ST, Dickson D, et al. The diagnosis of mild cognitive impairment due to Alzheimer's disease: recommendations from the National Institute on Aging-Alzheimer's Association workgroups on diagnostic guidelines for Alzheimer's disease. *Alzheimers Dement*. 2011;7:270–279.
5. Fischer P, Jungwirth S, Zehetmayer S, et al. Conversion from subtypes of mild cognitive impairment to Alzheimer dementia. *Neurology*. 2007;68:288–291.
6. Coppola G, Di Renzo A, Ziccardi L, et al. Optical coherence tomography in Alzheimer's disease: a meta-analysis. *PLoS One*. 2015;10:e0134750.
7. Knoll B, Simonett J, Volpe NJ, et al. Retinal nerve fiber layer thickness in amnestic mild cognitive impairment: case-control study and meta-analysis. *Alzheimers Dement (Amst)*. 2016;4:85–93.
8. Cheung CY, Ong YT, Hilal S, et al. Retinal ganglion cell analysis using high-definition optical coherence tomography in patients with mild cognitive impairment and Alzheimer's disease. *J Alzheimers Dis*. 2015;45:45–56.
9. Lad EM, Mukherjee D, Stinnett SS, et al. Evaluation of inner retinal layers as biomarkers in mild cognitive impairment to moderate Alzheimer's disease. *PLoS One*. 2018;13:e0192646.
10. Inman DM, Horner PJ. Reactive nonproliferative gliosis predominates in a chronic mouse model of glaucoma. *Glia*. 2007;55:942–953.
11. Ogden TE. Nerve fiber layer astrocytes of the primate retina: morphology, distribution, and density. *Invest Ophthalmol Vis Sci*. 1978;17:499–510.
12. Fernandez-Albarral JA, Salobrar-Garcia E, Martinez-Paramo R, et al. Retinal glial changes in Alzheimer's disease - a review. *J Optom*. 2019;12:198–207.
13. Ramirez AI, de Hoz R, Salobrar-Garcia E, et al. The role of microglia in retinal neurodegeneration: Alzheimer's disease, Parkinson, and glaucoma. *Front Aging Neurosci*. 2017;9:214.
14. Perez-Nievas BG, Serrano-Pozo A. Deciphering the astrocyte reaction in Alzheimer's disease. *Front Aging Neurosci*. 2018;10:114.
15. Grieshaber MC, Moramarco F, Schoetzau A, Flammer J, Orguel S. Detection of retinal glial cell activation in glaucoma by time domain optical coherence tomography. *Klin Monbl Augenheilkd*. 2012;229:314–318.
16. Ashimatey BS, King BJ, Swanson WH. Retinal putative glial alterations: implication for glaucoma care. *Ophthalmic Physiol Opt*. 2018;38:56–65.
17. Takayama K, Ooto S, Hangai M, et al. High-resolution imaging of the retinal nerve fiber layer in normal eyes using adaptive optics scanning laser ophthalmoscopy. *PLoS One*. 2012;7:e33158.
18. Scoles D, Higgins BP, Cooper RF, et al. Microscopic inner retinal hyper-reflective phenotypes in retinal and neurologic disease. *Invest Ophthalmol Vis Sci*. 2014;55:4015–4029.
19. McKhann GM, Knopman DS, Chertkow H, et al. The diagnosis of dementia due to Alzheimer's disease: recommendations from the National Institute on Aging-Alzheimer's Association workgroups on diagnostic guidelines for Alzheimer's disease. *Alzheimers Dement*. 2011;7:263–269.
20. Oboudiyat C, Gefen T, Varelas E, et al. Cerebrospinal fluid markers detect Alzheimer's disease in nonamnestic dementia. *Alzheimers Dement*. 2017;13:598–601.
21. Liu CC, Liu CC, Kanekiyo T, Xu H, Bu G. Apolipoprotein E and Alzheimer disease: risk, mechanisms and therapy. *Nat Rev Neurol*. 2013;9:106–118.
22. Monsell SE, Dodge HH, Zhou XH, et al. Results from the NACC Uniform Data Set Neuropsychological Battery Crosswalk Study. *Alzheimer Dis Assoc Disord*. 2016;30:134–139.
23. Gold DA. An examination of instrumental activities of daily living assessment in older adults and mild cognitive impairment. *J Clin Exp Neuropsychol*. 2012;34:11–34.
24. Johnson N, Barion A, Rademaker A, Rehkemper G, Weintraub S. The Activities of Daily Living Questionnaire: a validation study in patients with dementia. *Alzheimer Dis Assoc Disord*. 2004;18:223–230.
25. Weintraub S, Besser L, Dodge HH, et al. Version 3 of the Alzheimer Disease Centers' Neuropsychological Test Battery in the Uniform Data Set (UDS). *Alzheimer Dis Assoc Disord*. 2018;32:10–17.
26. Morris JC. The Clinical Dementia Rating (CDR): current version and scoring rules. *Neurology*. 1993;43:2412–2414.
27. Dubra A, Sulai Y. Reflective afocal broadband adaptive optics scanning ophthalmoscope. *Biomed Opt Express*. 2011;2:1757–1768.
28. Onishi AC, Roberts PK, Jampol LM, Nesper PL, Fawzi AA. Characterization and correlation of "Jampol dots" on adaptive optics with foveal granularity on conventional fundus imaging. *Retina*. 2019;39:235–246.
29. Schneider CA, Rasband WS, Eliceiri, KW. NIH Image to ImageJ: 25 years of image analysis. *Nat Methods*. 2012;9:671–675.
30. Koronyo-Hamaoui M, Koronyo Y, Ljubimov AV, et al. Identification of amyloid plaques in retinas from Alzheimer's patients and noninvasive in vivo optical imaging of retinal plaques in a mouse model. *Neuroimage*. 2011;54(suppl 1):S204–S217.
31. Tackenberg MA, Tucker BA, Swift JS, et al. Müller cell activation, proliferation and migration following laser injury. *Mol Vis*. 2009;15:1886–1896.
32. Edwards MM, Rodriguez JJ, Gutierrez-Lanza R, Yates J, Verkhratsky A, Lutty GA. Retinal macroglia changes in a

triple transgenic mouse model of Alzheimer's disease. *Exp Eye Res*. 2014;127:252–260.

33. Thomson KL, Yeo JM, Waddell B, Cameron JR, Pal S. A systematic review and meta-analysis of retinal nerve fiber layer change in dementia, using optical coherence tomography. *Alzheimers Dement (Amst)*. 2015;1:136–143.
34. Kwon JY, Yang JH, Han JS, Kim DG. Analysis of the retinal nerve fiber layer thickness in Alzheimer disease and mild cognitive impairment. *Korean J Ophthalmol*. 2017;31:548–556.
35. Kashani AH, Chen CL, Gahm JK, et al. Optical coherence tomography angiography: a comprehensive review of current methods and clinical applications. *Prog Retin Eye Res*. 2017; 60:66–100.
36. Jiang H, Wei Y, Shi Y, et al. Altered macular microvasculature in mild cognitive impairment and Alzheimer disease. *J Neuroophthalmol*. 2018;38:292–298.
37. Bulut M, Kurtulus F, Gozkaya O, et al. Evaluation of optical coherence tomography angiographic findings in Alzheimer's type dementia. *Br J Ophthalmol*. 2018;102:233–237.
38. Bailey TL, Rivara CB, Rocher AB, Hof PR. The nature and effects of cortical microvascular pathology in aging and Alzheimer's disease. *Neurol Res*, 2004;26:573–578.
39. Kisler K, Nelson AR, Montagne A, Zlokovic BV. Cerebral blood flow regulation and neurovascular dysfunction in Alzheimer disease. *Nat Rev*. 2017;18:419–434.
40. Zhang YS, Zhou N, Knoll BM, et al. Parafoveal vessel loss and correlation between peripapillary vessel density and cognitive performance in amnestic mild cognitive impairment and early Alzheimer's disease on optical coherence tomography angiography. *PLoS One*. 2019;14:e0214685.
41. Lambert JC, Heath S, Even G, et al. Genome-wide association study identifies variants at CLU and CR1 associated with Alzheimer's disease. *Nat Genet*. 2009;41:1094–1099.
42. Farrer LA, Cupples LA, Haines JL, et al. Effects of age, sex, and ethnicity on the association between apolipoprotein E genotype and Alzheimer disease. A meta-analysis. APOE and Alzheimer Disease Meta Analysis Consortium. *JAMA*. 1997; 278:1349–1356.
43. Mattsson N, Zetterberg H, Hansson O, et al. CSF biomarkers and incipient Alzheimer disease in patients with mild cognitive impairment. *JAMA*. 2009;302:385–393.
44. Hertze J, Minthon L, Zetterberg H, Vanmechelen E, Blennow K, Hansson O. Evaluation of CSF biomarkers as predictors of Alzheimer's disease: a clinical follow-up study of 4.7 years. *J Alzheimers Dis*. 2010;21:1119–1128.
45. Graf T, Flammer J, Prünte C, Hendrickson P. Gliosis-like retinal alterations in glaucoma patients. *J Glaucoma*. 1993;2:257–259.
46. Al Rashaed S, Khan A, Nowilaty S, Edward DP, Kozak I. Spectral-domain optical coherence tomography reveals prelaminar membranes in optic nerve head pallor in eyes with retinitis pigmentosa. *Graefes Arch Clin Exp Ophthalmol*. 2016;254:77–81.
47. Haritoglou C, Schumann RG, Wolf A. Epiretinal gliosis. *Ophthalmologe*. 2014;111:485–497.
48. Lombardo M, Scarinci F, Ripandelli G, et al. Adaptive optics imaging of idiopathic epiretinal membranes. *Ophthalmology*. 2013;120:1508–1509.e1.
49. Bosco A, Steele MR, Vetter ML. Early microglia activation in a mouse model of chronic glaucoma. *J Comp Neurol*. 2011;519: 599–620.
50. Williams PA, Marsh-Armstrong N, Howell GR; Lasker/IRRF Initiative on Astrocytes and Glaucomatous Neurodegeneration Participants. Neuroinflammation in glaucoma: a new opportunity. *Exp Eye Res*. 2017;157:20–27.
51. Grieshaber MC, Orgul S, Schoetzau A, Flammer J. Relationship between retinal glial cell activation in glaucoma and vascular dysregulation. *J Glaucoma*. 2007;16:215–219.
52. Alzheimer's Association. 2019 Alzheimer's disease facts and figures. *Alzheimers Dement*. 2019;15:321–387.
53. Sharma N, Singh AN. Exploring biomarkers for Alzheimer's disease. *J Clin Diagn Res*. 2016;10:KE01–KE06.
54. Handels RLH, Wimo A, Dodel R, et al. Cost-utility of using Alzheimer's disease biomarkers in cerebrospinal fluid to predict progression from mild cognitive impairment to dementia. *J Alzheimers Dis*. 2017;60:1477–1487.
55. Counts SE, Ikonomovic MD, Mercado N, Vega IE, Mufson EJ. Biomarkers for the early detection and progression of Alzheimer's disease. *Neurotherapeutics*. 2017;14:35–53.
56. Hinton DR, Sadun AA, Blanks JC, Miller CA. Optic-nerve degeneration in Alzheimer's disease. *N Engl J Med*. 1986;315: 485–487.

Investigative Ophthalmology & Visual Science